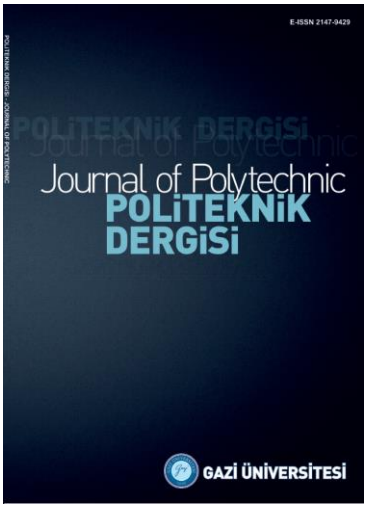

POLİTEKNİK DERGİSİ

JOURNAL of POLYTECHNIC

ISSN: 1302-0900 (PRINT), ISSN: 2147-9429 (ONLINE)
URL: http://dergipark.org.tr/politeknik

8 MHz high efficient resonant sepıc converter design for LED driver of endoscopy systems

Endoskopi sistemlerinin LED sürücüsü için 8 mhz yüksek verimli rezonans sepic dönüştürücü tasarımı

***Yazar(lar) (Author(s))**: Irem CORAK[1], Sevilay Cetin[2]*

ORCID[1]: 0000-0002-2920-124X

ORCID[2]: 0000-0002-9747-4821

To cite to this article: Corak I. and Cetin S., "8 MHz high efficient resonant sepıc converter design for led driver of endoscopy systems", ***Journal of Polytechnic***, 27(2): 461-468, (2024).

Bu makaleye şu şekilde atıfta bulunabilirsiniz: Corak I. and Cetin S., "8 MHz high efficient resonant sepıc converter design for led driver of endoscopy systems", ***Politeknik Dergisi***, 27(2): 461-468, (2024).

Erişim linki (To link to this article): http://dergipark.org.tr/politeknik/archive

DOI: **10.2339/politeknik.1118158**

8 MHz High Efficient Resonant SEPIC Converter Design for LED Driver of Endoscopy Systems

Highlights

- *High Efficiency*
- *SEPIC Converter*
- *LED Driver*
- *Endoscopic*

Graphical Abstract

In this work, a LED driver design based on resonant SEPIC converter is presented for using in Endoscopy Systems.

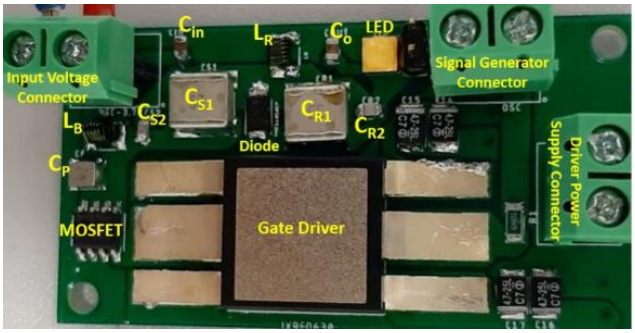

Figure. The picture of the built prototype.

Aim

In this work, high-efficiency and high-power density resonant SEPIC DC-DC converter design is aimed for light emitting diode (LED) driver of the LED integrated endoscopy device.

Design & Methodology

In the design procedure, low power consumption and low volume are taken into consideration. The operation frequency is selected high enough, 8 MHz, to provide high power density. First, a LED which has high power density, is determined to adapt the distal tip of an endoscopy device. Then, the design procedure presented in the literature is applied to the resonant SEPIC converter to drive selected LED.

Originality

In this work, the resonant SEPIC converter is designed for endoscopic LED driver with high efficiency and high power density. The design of the converter is carried out based on the voltage/current characteristic of a real high power density LED by Cree to be placed distal tip of an endoscopy device. The operation of the converter is provided at 8 MHz operation frequency while its peak efficiency is high enough as 84.5%.

Findings

The presented design was validated on a prototype and the output voltage is provided at 2.82 V to provide typical voltage of the LED while the load current is around 1 A.

Conclusion

According to obtained results, the peak efficiency is measured around 84.5% while the output voltage 2.82 V.

Declaration of Ethical Standards

The author(s) of this article declare that the materials and methods used in this study do not require ethical committee permission and/or legal-special permission.

8 MHz High Efficient Resonant SEPIC Converter Design for LED Driver of Endoscopy Systems

Araştırma Makalesi/Research Article

Irem CORAK*, Sevilay CETIN

Department of Biomedical Engineering, Technology Faculty, Pamukkale University, Turkey

(Geliş/Received : 18.05.2022 ; Kabul/Accepted : 02.08.2022 ; Erken Görünüm/Early View : 07.09.2022)

ABSTRACT

In this work, a light emitting diode (LED) driver design based on resonant SEPIC converter is presented for using in Endoscopy Systems. The resonant SEPIC converter operating with soft switching is good candidate to reduce the power consumption and increase the efficiency. In the design of the converter, the operation frequency is selected as 8 MHz in order to increase power density as well. The design of the converter is built based on voltage driven rectifier proposed in the literature to simplify the design procedure. Finally, the performance of the converter is verified on a prototype loaded with a LED, which has high power density. The maximum efficiency of the converter is measured around 84.5% while the output voltage is 2.82 V and the output current is around 1.02 A.

Key Words: LED Driver, SEPIC converter, high frequency, high efficiency.

Endoskopi Sistemlerinin LED Sürücüsü için 8 MHz Yüksek Verimli Rezonans SEPIC Dönüştürücü Tasarımı

ÖZ

Bu çalışmada, endoskopi sistemlerinde kullanılmak üzere rezonanslı SEPIC dönüştürücü tabanlı bir LED sürücü tasarımı sunulmaktadır. Yumuşak anahtarlama ile çalışan rezonanslı SEPIC dönüştürücü, güç tüketimini azaltmak ve verimliliği artırmak için iyi bir alternatiftir. Dönüştürücünün tasarımında güç yoğunluğunu artırmak için çalışma frekansı 8 MHz olarak seçilmiştir. Dönüştürücünün tasarımı, tasarım prosedürünü basitleştirmek için literatürde önerilen gerilim tahrikli doğrultucu temel alınarak yapılmıştır. Son olarak, dönüştürücünün performansı, LED yüklü yüksek güç yoğunluğuna sahip bir prototip üzerinde doğrulanmıştır. Dönüştürücünün maksimum verimi %84,5 civarında ölçülürken çıkış gerilimi 2,82 V ve çıkış akımı 1,02 A civarındadır.

Anahtar Kelimeler: LED sürücü, SEPIC dönüştürücü, yüksek frekans, yüksek verimlilik.

1. INTRODUCTION

Endoscopy systems are widely used to observe tissues and internal organs. They can also be used in minimally invasive surgery (MIS) and imaging in the diagnosis and treatment of diseases [1].

An endoscopy system includes illumination and imaging units. In the conventional endoscopy system, the light is directed from an external source to the tip of the endoscopy device, while the imaging optics captures the light reflected from the surgical field and directs it to the processing of images [2]. The light is directed to the tip of endoscopy device by a fiber bundle, which is connected to the external light source with limited acceptance angle. Therefore, the most of the light is lost due to the way of the connection. Besides, an infrared heat energy caused by fiber bundle can be transmitted to the patient and results in danger during the process [3-5]. The overall efficiency of the systems including an external light source and endoscope is around 16%-19% as well [2]. Therefore, there is a need for integrated new systems to replace external light sources in endoscopy systems.

The xenon, halogen or light emitting diodes (LEDs) are usually used as endoscopic light source. However, xenon and halogen lamps generate a lot of heat, they are expensive and short-lived. Approximately 300 W electrical power is needed to provide only 1 W optical power [6]. Recently, LEDs have started to replace halogen and xenon lamps for endoscopic light source [3, 6]. LEDs have entered the lighting industry and provided noticeable advantage in terms of energy saving [7]. They can be integrated into the endoscope system due to their small volume. Thus, closer light source to the processing area can be obtained. In addition, LEDs have advantages of low cost, light weight, high energy saving and low heat generation compared to xenon and halogen lamps for endoscopy systems [5].

*Sorumlu yazar(Corresponding Author)
e-mail : scetin@pau.edu.tr

For safe operation of LEDs, drivers controlling the current and the voltage of LEDs are required. It is also important that LED drivers should be designed to not limit the performance of the LED [8]. Therefore, design stage of the selected driver topology is important task to provide the best performance of the LED. The power converters are usually used for LED drive process. The low power consumption, high efficiency, high power density and thermal management are the key issues for the power converters designed to be used as LED drivers in the endoscopy system.

In the power converters, the most of the volume is usually occurred by passive components which are reducing the power density [9-11]. Therefore, the operation of the selected LED driver at high frequency is required to provide small volume and high power density. The stored energy in the passive components reduces at high switching frequency due to their reduced volume and values [12, 13]. However, operation at high frequency increases the switching losses causing lower efficiency. Thus, in order to reduce or eliminate the switching losses, the use of soft switching techniques or soft switched converters is unavoidable [14, 15]. The soft switching techniques keep the voltage across the power semiconductors at a very low level during the turn-on and turn-off transitions [16-19]. The recovering the energy stored in the output capacitance of the power semiconductor plays important role to increase the efficiency at high operation frequency [16, 20].

In the resonant converter topologies, the output capacitance of the power semiconductor switches can be discharged by resonance [9, 21-23]. Thus, switching losses are minimized or eliminated at high operation frequency.

One of the resonant converter topologies, the LLC resonant converter has the advantage of zero voltage switching (ZVS) for all load conditions in inductive operation region [24], [25]. High frequency inductor-inductor-capacitor (LLC) resonant converter applications are presented in [22-27]. As seen in these studies, LLC resonant converters have high efficiency, but their magnetic components are complex and bulky. It is not suitable for low power applications and is costly. Also, not having a ground referenced switch reduces the reliability of the drive circuit. The circuit topologies, which have active switches with ground reference, are usually preferred in high frequency applications. [9, 28].

Among the resonant converters, the resonant SEPIC converter, class E resonant converter, resonant boost converter and class Φ^2 resonant converter have ground-referenced switch. When these converters evaluated based on [9], [12], [28] and [29], resonant SEPIC converter is more advantageous at high operation frequency compared to the others. Because the resonant SEPIC converter does not include a bulk inductor and operates at constant operation frequency. Thus, it has improved response speed and allows low loss resonant gate drive [30]. Based on these features, in this work, resonant SEPIC converter is selected to drive the LED of an endoscopy system.

The resonant SEPIC converter applications have been presented in different works, in the literature [9], [21], [28], [30]-[33]. In [9], a new design method is presented for the high frequency resonant SEPIC converter operating at 30 MHz. The new design procedure redivided the resonant SEPIC topology into two subsystems to provide independent tuning the amplitude and the phase. In this way, the voltage-driven rectifier with series capacitor replaces the current-driven rectifier and the design is simplified. The analysis and design procedure of a self-oscillating resonant SEPIC converter that can operate at very high frequencies ranging from 30 MHz to 300 MHz is presented in [21]. The presented circuit has complex design which is built with two resonant SEPICs and required an interconnection network. In [28], a SEPIC converter design method and its control are presented to provide operation at very high frequencies. The proposed method allows high efficiency over wide input and output voltage range. In [30], different SEPIC topologies are discussed and the superiority of the resonant SEPIC topology over other SEPIC topologies is explained, and simulation results are presented. In [33], a self-oscillating SEPIC converter is proposed for LED drive application. The use of the phase shift burst mode control method make the control circuity of the converter complicated. The peak efficiency is obtained around %81 at 10.5 W power rate. In order to reduce voltage stress of the semiconductors and increase the voltage transformation ratio, another self-oscillating SEPIC converter is proposed in [34]. The target of the method is provided with the use of additional component in conventional SEPIC converter. In [35], a quasi-resonant converter is discussed in terms of distributed maximum power point trackers. The maximum efficiency of the converter is evaluated in a medium frequency range. In [36], ZVS resonant SEPIC converter is evaluated for photovoltaic applications. The closed-loop operation of the converter is tested by simulation.

In this work, high-efficiency and high-power density resonant SEPIC converter design is proposed for LED driver of the LED integrated endoscopy device. In the design procedure, low power consumption and low volume are taken into consideration. First, a LED which has high power density, is determined to adapt the distal tip of an endoscopy device. Then, the design procedure presented in [9] is applied to the resonant SEPIC converter to drive selected LED. The spotlight of this paper is the carrying out the high efficiency design of the converter based on the voltage and current characteristic of a real high power density LED by Cree, to be placed to the distal tip of the endoscopy device. The obtained design procedure was validated on a prototype which has 2.82 V output voltage and 1.02 A output current. The operation of the converter was provided at 8 MHz operation frequency while its efficiency is high enough. According to the obtained results, the peak efficiency

was measured around 84.5% while the output voltage is 2.82 V.

2. PRINCIPLES OF THE RESONANT SEPIC CONVERTER

The circuit diagram of the resonant SEPIC converter is given in Figure 1. The circuit topology of the resonant SEPIC converter is similar with the conventional SEPIC converter in [37] and with the multi resonant SEPIC converter given in [38]. However, component size, operation principle and placement of the component in the resonant SEPIC converter are very different. The conventional SEPIC converter operates with hard switching and has two bulk inductors. The multiresonant SEPIC converter also has bulk inductors but it achieves ZVS for the switch and diode. The resonant SEPIC converter requires only two inductors as shown in Figure 1. The resonant SEPIC converter operates at the constant operation frequency and duty ratio [28, 30] with the use of on/off control. Thus, bulky inductors are eliminated compared to previous designs presented in [37] and [38].

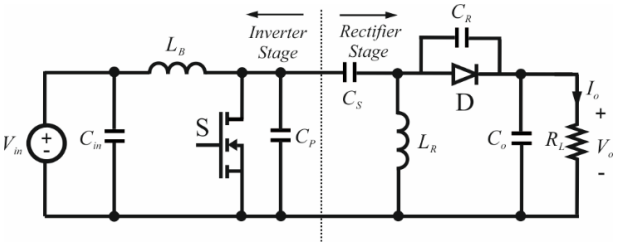

Figure 1. The resonant SEPIC Converter.

The operation of the resonant SEPIC converter can be simplified with two subsystems which are inverter stage and the rectifier stage [9]. According to the design procedure given in [9], V_{in} input source, C_{in} input filter capacitor, L_B filter inductor, S MOSFET and C_P resonant capacitor consisting of the parasitic capacitor of the S MOSFET constitute the inverter stage. The rectifier stage includes D diode, L_R resonant inductor, C_o filter capacitor, C_R resonant capacitor, C_S series capacitor and R_L load. Finally, V_o is the output voltage. These two subsystems can be given in Figure 2 and Figure 3, as presented in [9]. The key waveforms representing operation of the resonant SEPIC converter is given Figure 4.

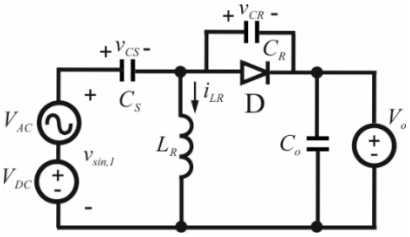

Figure 2. The voltage driven rectifier stage of resonant SEPIC converter.

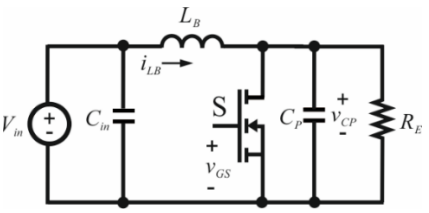

Figure 3. Inverter stage of resonant SEPIC converter.

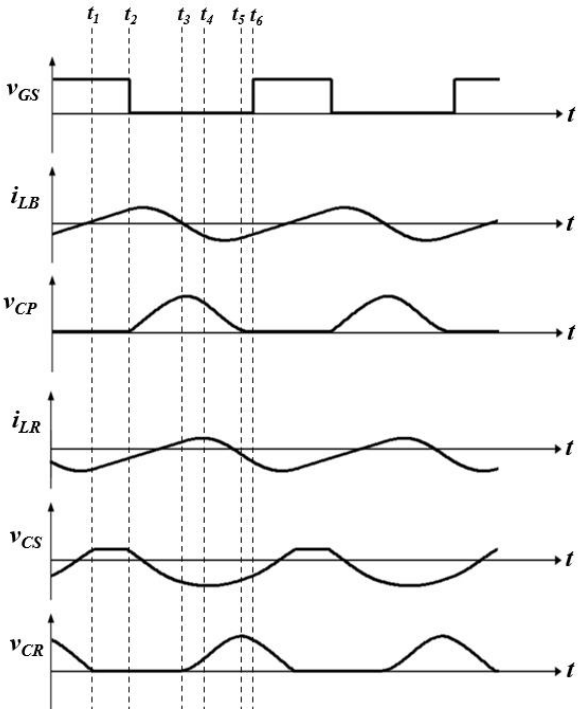

Figure 4. The operational key waveforms of the resonant SEPIC converter.

In the voltage driven rectifier stage, there are three resonant components which are L_R, C_R and C_S. A resonance occurs between C_S, L_R and C_R while S MOSFET is on and D diode is off condition. In the resonance operation, the voltage of the diode, V_{CR}, smoothly decreases and the current of L_R discharges while the voltage of C_S increases. At $t=t_1$, V_{CR} reaches zero, V_{CS} charges to the output voltage and so S MOSFET is turned-off and D diode is turned-on, at $t=t_2$. With the conduction of the D diode, the voltage across the L_R becomes positive and its current starts to increase. When the current of L_R exceeds the input current of the rectifier, D diode is turned-off at $t=t_3$. After the turn-off of diode, the voltage of C_R capacitor smoothly starts to increase while the voltage of C_S capacitor continue to increase in inverse direction. At $t=t_4$, i_{LR} reaches its maximum value while C_S reaches own maximum in negative direction. Then, L_R starts to discharge, V_{CR} reaches its maximum at $t=t_5$. At $t=t_6$ S MOSFET is on again and cycle repeats. The resonant frequency $f_{o\text{-}rec}$ and the characteristic impedance $Z_{o\text{-}rec}$ can be defined, based on [9], as follows:

$$f_{o-rec} = \frac{1}{2\pi\sqrt{L_R(C_S+C_R)}} \quad (1)$$

$$Z_{o-rec} = \sqrt{\frac{L_R}{C_R+C_S}} \quad (2)$$

In the inverter stage, rectifier stage represented by R_E equivalent resistance and there are two resonant components which are L_B and C_P, as shown in Figure 3. Based on [9], the equivalent resistance of the rectifier stage, R_E, can be written, as follows:

$$R_E = \frac{8V_{in}^2}{\pi^2} \cdot \frac{1}{P_{in}} \quad (3)$$

Where P_{in} is the input power of the rectifier stage. When the S MOSFET is turned-off, a resonance occurs between L_B and C_P. In order to achieve ZVS for S MOSFET, inductive operation should be provided. For this purpose, resonance frequency can be set by

$$f_{o-inv} = \frac{1}{2\pi\sqrt{L_B C_P}}. \quad (4)$$

When the S MOSFET is off condition, the equivalent circuit across the MOSFET shows parallel characteristic including L_B, C_P and R_E. Thus, switching frequency below resonant frequency provides ZVS for the MOSFET. During the turn-off of the MOSFET, the voltage of C_P smoothly increases while the current of L_B decreases and the current of L_R increases. When the current of L_B reaches zero, the voltage of C_P reaches its maximum value, at $t=t_3$. Then, C_P capacitor starts to discharge while the current of L_B is increasing in negative direction. When the voltage of C_P reaches zero, at $t=t_5$, the body diode of the MOSFET turns-on to achieve ZVS turn-on for the MOSFET. During the turn-on of the MOSFET, L_B inductor stores the energy for the determined time.

3. DESIGN OF THE RESONANT SEPIC LED DRİVER

In the conventional design procedure given in [28], current driven rectifier causes serious coupling between resonant frequency and resonant impedance [9]. Although this design procedure seems easy, it is quite difficult to achieve ZVS, it requires a lot of optimization work. Therefore, design procedure using voltage driven rectifier proposed in [9] is used in this work. In the voltage driven rectifier, the power factor and output power can be designed independently, which simplifies the design. The inverter stage contains only two resonant components. This simplifies the design of the inverter stage as well.

In the design of LED driver, the input voltage is selected as 3.7 V taking into consideration the feeding from a Li-ion battery. For the load of the resonant SEPIC converter, a LED with high power density (XLamp XP-L2 from Cree) is selected. According to determined LED datasheet, the typical voltage is around 2.82 V while its current is 1050 mA.

Based on given design procedure in [9], circuit components of the resonant SEPIC converter for the LED driver are determined as given in Table I. The switching frequency is selected as 8 MHz to provide high power density. In order to achieve ZVS for the MOSFET, inverter resonant frequency is around 27.7 MHz based on equation (4). Resonant SEPIC converter design is realized by combining the designed inverter and rectifier. Different results can be seen in circuit waveforms and output power level due to the non-linear interaction between the two stages. Additional settings can be made by changing resonant component's value to achieve soft switching and the required power level.

Table 1. The determined design parameters of the proposed resonant SEPIC converter.

Parameters	Value
L_B	33 nH
C_P	1 nF
C_S	5.9 nF
C_R	5 nF
L_R	33 nH
C_o	47 µF
C_{in}	4.7 µF
V_{in}	3.7 V
V_o	2.82 V
I_o	1050 mA

4. SIMULATION AND EXPERIMENTAL RESULTS

4.1. Simulation Results

The operation of the converter is firstly tested with a simulation work implemented by PSIM. The LED is modeled with a resistor and Zener diode at the load side. The determined design parameters mentioned earlier were used in the simulation work. The output voltage of the converter and gate-source voltage of the power MOSFET, V_{GS}, are shown in Figure 5. According to obtained results, 2.8 V output voltage and 1.09 A output current were provided with simulation work. The ZVS operation of the power MOSFET was also tested by simulation as shown in Figure 6. The power MOSFET is turn-on with ZVS, while the drain-source voltage of the power MOSFET, v_{DS}, is zero

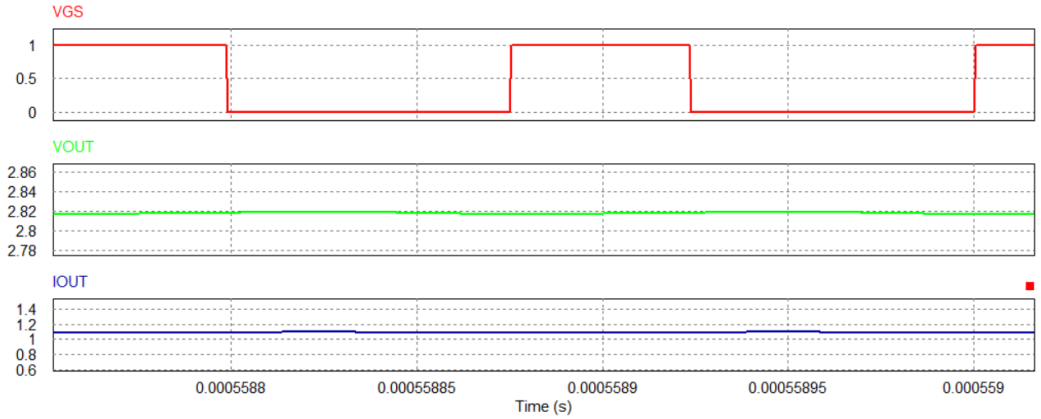

Figure 5. The simulated gate-source voltage of the power MOSFET, output voltage and the output current waveforms of the converter.

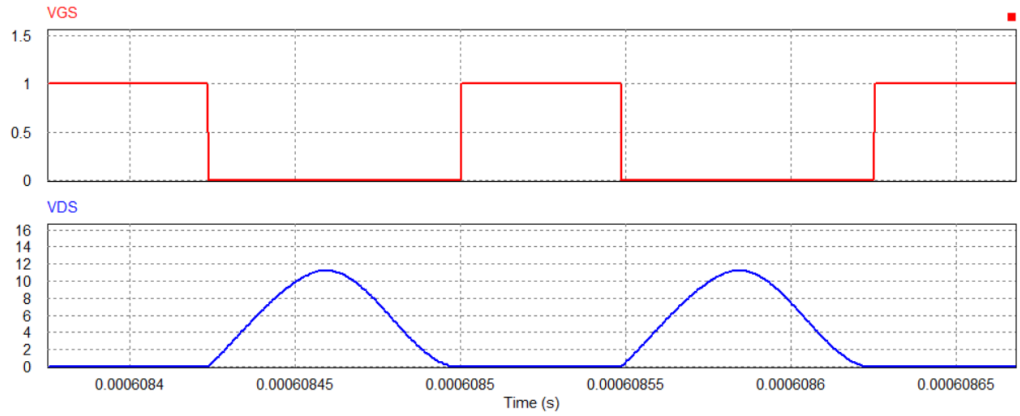

Figure 6. The simulated gate-source voltage, v_{GS}, and drain-source voltage, v_{DS}, of the MOSFET.

4.2. Experimental Results

The operation of the resonant SEPIC converter is validated by a prototype built with the design parameters given in Table I. In the determination of the power semiconductors, IRF7473Pbf and PMEG4050EP are used for the power MOSFET and rectifier diodes. To drive power MOSFET, IXRFD630 gate drive is used. An open loop control circuit is design for the power control of the converter. A signal generator is used to produce 8 MHz pulse width modulated (PWM) signals. Then, a gate driver which has high frequency drive capacity, is used to drive the power MOSFET. The IXRFD630, producing 30 A of peak current, was determined as the gate driver. The picture of the built prototype is given in Figure 7.

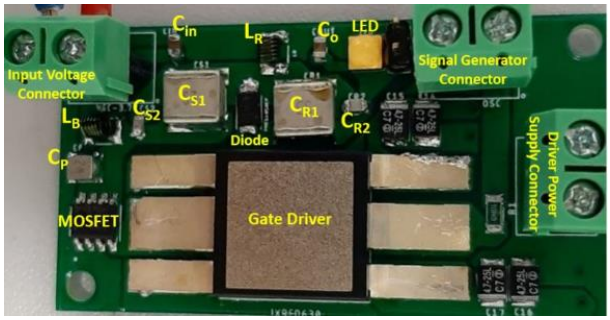

Figure 7. The picture of the built prototype.

The measured waveforms of the output voltage and gate-source voltage of the power MOSFET are given in Figure 8. As shown in Figure 8 (a), the output voltage at 2.8 V is experimentally provided while the duty ratio is 0.35 and the output current is 1.02 A. Figure 8 (b) shows 320 mV measured ripple on the output voltage. The ripple can be minimized further with the use of larger filter capacitor at the output of the converter.

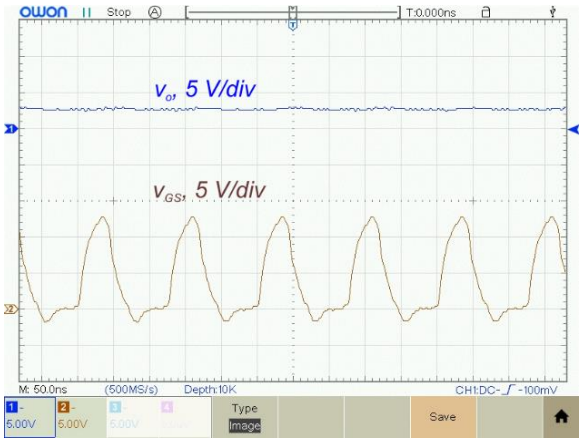

(a)

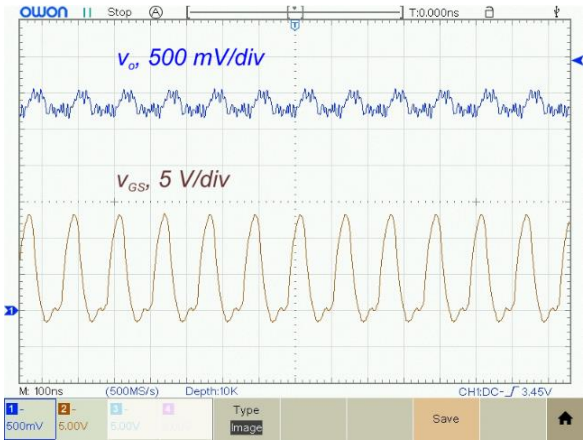

(b)

Figure 8. The output voltage waveforms. (a) The measured output voltage at 2.8 V. (b) The output voltage ripple around 320 mV. The output current is 1.02 A, duty ratio is 0.35.

The gate-source voltage, v_{GS}, and drain-source voltage, v_{DS}, of the MOSFET, while the duty ratio is 0.35, are measured as given in Figure 9. According to measured results, the power MOSFET operates with soft switching. The measured diode voltage, v_D, is given in Figure 10. The peak reverse voltage of the diode is measured around 10 V.

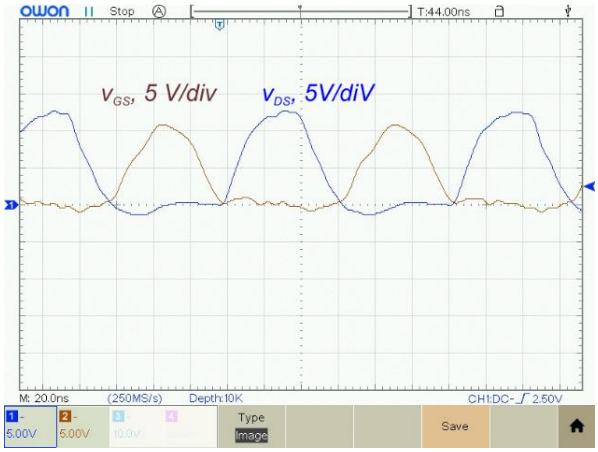

Figure 9. The gate-source voltage, v_{GS}, and drain-source voltage, v_{DS}, of the MOSFET.

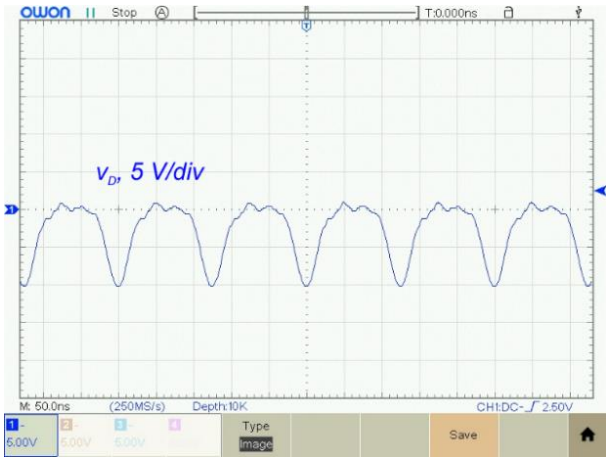

Figure 10. The waveforms of the rectifier diode voltage, v_D.

The efficiency performance of the converter is also tested on the built prototype. The maximum efficiency is measured around 84.5% while the output voltage is 2.82 V and the output current is around 1.02 A. The efficiency variation based on LED voltage was given in Figure 11. The LED starts to heat up in proportion to the power consumed on it. The efficiency was decreased while the LED voltage is reducing due to the temperature increase.

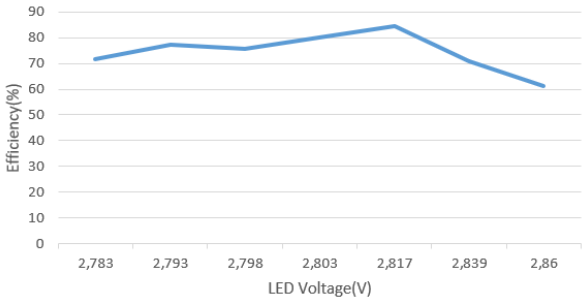

Figure 11. The measured efficiency variation of the converter as function of LED voltage.

6. CONCLUSION

In this paper, a LED driver design for an endoscopy system is presented. In order to provide high efficiency, resonant SEPIC converter operating with soft switching is used to drive the LED. The operation frequency is selected high enough, 8 MHz, to provide high power density. The design procedure, which is including inverter and rectifier stage, of the resonant SEPIC converter is built based on the methods proposed in literature. Finally, a prototype is built to validate the operation of the LED driver. A real LED with high power density is used as load at the output of the converter. The output voltage is provided at 2.82 V to provide typical voltage of the LED while the load current is around 1.02 A. According to measured results, the maximum efficiency of the converter is measured as 84. 5%.

ACKNOWLEDGEMENT

This work is supported by Pamukkale University under grant number 2021FEBE013.

DECLARATION OF ETHICAL STANDARDS

There is no need to obtain permission from the ethics committee for the article prepared. There is no conflict of interest with any person/institution in the article prepared.

AUTHORS' CONTRIBUTIONS

Irem Corak: She put contribution in literature searching, analyzing of the SEPIC converter. She also built the prototype and measured the current, voltage and efficiency results of the SEPIC converter.

Sevilay Cetin: She put contribution in the creating idea of the paper and managing the all stages in the paper.

CONFLICT OF INTEREST

There is no conflict of interest in this study.

REFERENCES

[1] Smith T., "Endoscopy. British Medical Association Complete Family Health Encyclopedia", ***Dorling Kindersley Ltd.***, 403-404, (1990).

[2] Gärtner A, Belloni P., "Optical designs to improve LED lighting efficiency of medical endoscopes", ***LED Professional***, https://www.led-professional.com/resources-1/articles/optical-designs-to-improve-led-lighting-efficiency-of-medical-endoscopes, (2020).

[3] Brüggemann, D., Blase, B., Bühs, F., Dreyer, R., Kelp, M., Lehr, H., Oginski, S. and Schlegel, S., "Endoscope with distal LED for illumination", ***World Congress on Medical Physics and Biomedical Engineering***, ***Springer Berlin Heidelberg,*** Beijing/China, 2107-2110, (2012).

[4] Hensman C., Hanna G.B., Drew T., Moseley H. and Cuschieri A., "Total radiated power, infrared output, and heat generation by cold light sources at the distal end of endoscopes and fiber optic bundle of light cables", ***Surgical Endoscopy***, 12(4): 335–337, (1998).

[5] Todd E.F.D., Ertas H. and Hamel A.J., "Disposable attachable light source unit for an endoscope", ***US8029439B2 United States Patent***, (2005).

[6] Clancy N.T., Li R., Rogers K., Driscoll P., Excel P., Yandle R. and Elson D.S., "Development and evaluation of a light-emitting diode endoscopic light source", ***Advance Biomedical and Clinical Diagnostic Systems***, 8214: 82140R-1- 82140R-7, (2012).

[7] Govind B.N. and Dhoble S.J., "The fundamentals and applications of light-emitting diodes", ***Woodhead Publishing,*** 35-56, (2020).

[8] Lamar D.G., "Latest developments in LED drivers", ***Electronics***, 9(4): 619, 2020.

[9] Zhang Z., Lin J., Zhou Y. and Ren X., "Analysis and decoupling design of a 30 MHz resonant SEPIC converter", ***IEEE Transactions on Power Electronics***, 31(6): 4536-4548, (2016).

[10] Shen W., Wang F., Boroyevich, D. Tipton, C.W., "High-density nanocrystalline core transformer for high-power high-frequency resonant converter", ***IEEE Transactions on Industry Applications***, 44(1): 213-222, (2008).

[11] Li B., Li Q., Lee F.C., "High-frequency PCB winding transformer with integrated inductors for a bi-directional resonant converter", ***IEEE Transactions on Power Electronics***, 34(7): 6123-6135, (2019).

[12] Wang Y., Lucia O., Zhang Z., Gao S., Guan Y. and Xu D., "A review of high frequency power converters and related technologies", ***IEEE Open Journal of the Industrial Electronics Society***. 1: 247-260, (2020).

[13] Guan Y., Liu C., Wang Y., Wang W. and Xu D., "Analytical derivation and design of 20-Mhz dc–dc soft-switching resonant converter", ***IEEE Transactions on Industrial Electronics***, 68(1): 210-221, 2021.

[14] Cetin S. "An improved zero voltage transition PWM boost converter with an active snubber cell", ***Journal of Circuit, Systems, and Computers***, 25(10): 1650128-1, 1650128-23, (2016).

[15] Cetin S. "High efficiency design considerations for the self-driven synchronous rectified phase-shifted full-bridge converters of server power systems", ***Journal of Power Electronics***, 15(3): 634-643, (2015).

[16] Rivas J.M., Jackson D., Leitermann O., Sagneri A.D., Han Y., Perreault D.J., "Design considerations for very high frequency dc-dc converters", ***37th IEEE Power Electronics Specialists Conference,*** Jeju/Korea(South), 1-11, (2006).

[17] Lee F.C., "High-frequency quasi-resonant converter technologies", ***Proceedings of the IEEE***, 76: 377-390, (1988).

[18] Cetin S., "Power factor corrected and fully soft switched PWM boost converter", ***IEEE Transactions on Industry Applications***, 54(4): 3508-3517, (2018).

[19] Nour Y., Knott A. and Petersen L.P., "High frequency soft switching half bridge series-resonant DC-DC converter utilizing gallium nitride FETs", ***19th European Conference on Power Electronics and Applications***, 1-7, (2017).

[20] Zulauf G., Tong Z., Plummer J.D. and Rivas-Davila J.M., "Active power device selection in high- and very-high-frequency power converters", ***IEEE Transactions on Power Electronics***, 34(7): 6818-6833, (2019).

[21] Kovacevic M., Knott A. and Andersen M.A.E., "Very high frequency interleaved self-oscillating resonant SEPIC converter", ***15th European Conference on Power Electronics and Applications,*** Lille/France, 1-9, (2013).

[22] Li M., Ouyang Z., Andersen M.A.E., "High frequency LLC resonant converter with magnetic shunt integrated planar transformer", ***IEEE Applied Power Electronics Conference and Exposition***, San Antonio/USA, 2678-2685, (2018).

[23] Fei C., Gadelrab R., Li Q., Lee F.C., "High-frequency three-phase ınterleaved LLC resonant converter with GaN devices and integrated planar magnetics", ***IEEE Journal of Emerging and Selected Topics in Power Electronics***, 7(2): 653-663, (2019).

[24] Cetin S., Yenil V., "Optimal operation region of LLC resonant converter for on-board EV battery charger applications", ***IEEE 18th International Conference on Power Electronics and Motion Control Conference***, Budapest/Hungry, 78-85, (2018).

[25] Oncu S., Nacar S., "Investigation of the effects of different operating regions of ZVS LLC resonant converter on the converter performance", ***Journal of Polytechnic***, Early Access, DOI: 10.2339/ politeknik.1089364, (2022).

[26] Khatua M., Shahzad D., Pervaiz S., Afridi K.K., "A high-power-density electrolytic-free offline LED driver utilizing a merged energy buffer architecture", ***IEEE Applied Power Electronics Conference and Exposition,*** Anaheim/USA, 768-773, (2019).

[27] Kim K., Youn H., Baek J., Jeong Y. and Moon G., "Analysis on synchronous rectifier control to improve regulation capability of high-frequency LLC resonant converter", ***IEEE Transactions on Power Electronics***, 33(8): 7252-7259, (2018).

[28] Jingying H., Sagneri A.D., Rivas J.M., Yehui H., Davis S.M. and Perreault D.J., "High frequency resonant SEPIC converter with wide input and output voltage ranges", ***IEEE Transactions on Power Electronics***, 27(1): 189-200, (2012).

[29] Yilmaz S., Sazak B.S. and Cetin S., "Design and implementation web-based training tool for a single switch induction cooking system using PHP", ***Elektronika ir Elektrotechnika***, 99: 89-92, (2010).

[30] Jose R., Shivanandan A. and Venugopal V., Devi K. "DC-DC SEPIC converter topologies", ***International Journal of Research in Engineering and Technology***, 4: 20-23, (2015).

[31] Madsen M.P., Knott A. and Andersen M.A.E. "Very high frequency resonant DC/DC converters for LED lighting", ***Twenty-Eighth Annual IEEE Applied Power Electronics Conference and Exposition***, Long Beach/USA, 835-839, (2013).

[32] Vadivoo R.S., Maheswari L., Vijayalakshmi S. and Vairamani K., "Design and modeling of ZVS resonant SEPIC converter for high frequency applications", ***International Conference on Circuits, Power and Computing Technologies***, Nagercoil/India, 873-880, (2014).

[33] Kovacevic M., Knott A. and Andersen M.A.E. "A VHF interleaved self-oscillating resonant SEPIC converter with phase-shift burst-mode control", ***IEEE Applied Power Electronics Conference and Exposition***, Fort Worth/USA, 1402-1408, (2014).

[34] Kovacevic M., Knott A. and Andersen M.A.E. "VHF series-input parallel-output interleaved self-oscillating resonant SEPIC converter", Denver/USA, ***IEEE Energy Conversion Congress and Exposition,*** Denver/USA, 2052-2056, (2013).

[35] Duman, T. and Boztepe, M., "Evaluation of zero voltage switching SEPIC converter for module integrated distributed maximum power point tracking applications", ***10th International Conference on Electrical and Electronics Engineering (ELECO)***, Bursa/Turkey, 1480-1484, (2017).

[36] Saravanan, S., UshaRani, P., "Modeling and Control of Solar PV System with Closed Loop ZVS Resonant SEPIC Converter", ***International Journal of Innovative Technology and Exploring Engineering (IJITEE)***, 9: 152-156, (2019).

[37] Erickson R.W. and Maksimovic D., "Fundamentals of Power Electronics", ***Springer***, Boston, MA, (2001).

[38] Tabisz W. and Lee F., "Zero-voltage-switching multiresonant technique: A novel approach to improve performance of high-frequency quasi-resonant converters", ***IEEE Transactions on Power Electronics***, 4(4), 450–458, (1989)